# Unfolding and Refolding of Sol−Gel Encapsulated Carbonmonoxymyoglobin: An Orchestrated Spectroscopic Study of Intermediates and Kinetics†

**U. Samuni, M. S. Navati, L. J. Juszczak, D. Dantsker, M. Yang, and J. M. Friedman***

*Department of Physiology and Biophysics, Albert Einstein College of Medicine, Bronx, New York 10461*

*Received: February 24, 2000; In Final Form: May 24, 2000*

The pH-induced unfolding and refolding of the carbon monoxide-bound derivative of horse skeletal myoglobin (COMb) encapsulated in porous sol−gels is probed using several optical techniques in conjunction with different unfolding/refolding protocols. UV resonance Raman (UVRR) spectroscopy and fluorescence are used to monitor the unfolding of the globin and exposure of the A helix to solvent. Absorption spectra, visible resonance Raman (VRR) spectra, and geminate recombination are used to probe the heme and the heme environment. Encapsulation slows the kinetics of acid-induced unfolding and dramatically slows the kinetics of refolding. The spectra and the kinetics imply that this approach allows for the detailed study of the burst phase of unfolding. Using different encapsulation protocols and sequences of solvent replacements, it is possible to trap and probe not only low-pH forms observed in solution-phase studies but also novel partially unfolded species that are likely to be important unfolding and folding intermediates. The role of water as a chaotropic agent is indicated by the spectral changes that occur in the introduction and subsequent removal of glycerol from the solution bathing the unfolded and partially unfolded, sol−gel encapsulated COMb. The results directly support the view that unfolding or increasing the exposure to solvent of at least some segment of the A helix is the initial step in the unfolding pathway. In addition, the results indicate that the refolding of the A helix is likely to be the last process in the refolding pathway.

## I. Introduction

How proteins fold and unfold is an important biophysical question that is the focus of a considerable effort on the part of the research community. Two general approaches are often used in pursuing this problem. In one instance, denaturant or renaturant is systematically added to a protein solution in order both to generate a titration curve that exposes the stability of a given species and to reveal the existence of intermediates. In the other approach, a protein solution is rapidly mixed with a second solution that initiates either unfolding or refolding. In such studies, the objectives include monitoring of the kinetics of the process and spectroscopic identification of the unfolding or folding intermediates. Both the titration and kinetic approaches have limitations with respect to achievement of one of the central objectives in this area of research: identification and characterization of transition states for the unfolding and folding process. The often-complex mix of intermediates in titration studies, the short lifetime of the transition state as well as other key intermediates, and the temporal limitations in a rapid-mixing experiment all contribute to the difficulty in studying intermediates. In the present study, the unfolding and refolding of sol−gel encapsulated carbonmonoxymyoglobin (COMb) is studied using several spectroscopic probes in a concerted fashion. The findings indicate that sol−gel encapsulated proteins are a promising system not only for controlling the kinetics of the unfolding and refolding processes, but also for trapping and characterizing unstable forms that are likely candidates for transition state species.

It has been shown that many proteins can be encapsulated in porous sol−gels derived from either tetramethyl or tetraethyl orthosilicate (TMOS or TEOS, respectively) with a retention of native structure, functionality, and enhanced stability.[1−11] The sol−gel matrix traps the protein, but solvent, ions, and other small solute molecules can diffuse into the sol−gel through a network of 50−100 Å diameter pores. Small molecules can bind to or react with the encapsulated protein. Thus, for example, encapsulated myoglobins and hemoglobins can be easily and reversibly liganded, reduced, and oxidized by addition of appropriate reactants to the solution bathing the sol−gel.[1,9,11]

Studies of encapsulated hemoglobin (Hb) have shown that the sol−gel matrix greatly limits conformational changes.[12−17] Oxygen titration studies revealed an absence of cooperative binding for samples initially prepared as encapsulated oxyHb or deoxyHb.[12−15] The former reversibly bound oxygen with high affinity, whereas the latter bound oxygen with low affinity. The results were consistent with the Hb being trapped in either the high-affinity R or the low-affinity T quaternary conformation. Subsequent visible[16] and UV[17] resonance Raman studies not only confirmed the locking in of the initial structure via encapsulation but also showed that, by controlling the temperature of the sol−gel, one could systematically tune the rate of both tertiary and quaternary structural change. The sol−gel can affect conformational changes of the protein to a point where they are slower than the diffusion time of an added substrate. Thus, the sol−gel provides a method of overcoming the mixing and diffusion limitations associated with traditional rapid-mix and stopped-flow techniques.

The ability to use the sol−gel as a means of overcoming the diffusion limitations in rapid-mix experiments, coupled with the properties of sol−gels that eliminate protein aggregation but

† Part of the special issue "Thomas Spiro Festschrift".

* Author to whom correspondence should be addressed. Department of Physiology and Biophysics, Albert Einstein College of Medicine, Bronx, NY 10461. Phone: 718 430 3591. Fax: 718 430 8819. E-mail: jfriedma@aecom.yu.edu.

10.1021/jp000802g CCC: $19.00 
Published on Web 07/06/2000

allow for extreme yet facile variation in solution conditions, raises the prospect of using encapsulated proteins to study unfolding and refolding processes. Previous measurements[7] indicated that encapsulated proteins could be reversibly denatured in some instances, but the issue was not addressed systematically. In the present study, a more systematic and extensive study was pursued. Mb was chosen for study in the present work because the structure and function of Mb are well characterized over the required wide range of solution conditions. Both holo and apo myoglobins have been extensively used in studies of unfolding/folding. Both proteins are associated with a rich database that can provide a framework for comparing and understanding the corresponding processes occurring within the sol−gel.

The holo form offers a spectroscopic advantage in that the absorption and Raman spectra of the heme provide details regarding the conformational status of the helices that comprise the heme pocket. Recent UV resonance Raman studies of acid-induced unfolding of holo[18] and apo[19] Mb suggest that, with respect to certain domains, both proteins adopt similar acid-unfolded structures.

In the present study, the focus is primarily on encapsulated COMb. COMb offers several additional advantages over other forms of holoMb. It can be photodissociated using a short laser pulse. The 8-ns quantum yield for photodissociation and the nanosecond-to-microsecond geminate rebinding are highly responsive to the integrity of both the distal and the proximal heme environment, thus providing an additional probe of a local conformational coordinate during the unfolding and refolding cycle. Moreover, the visible resonance Raman spectrum of the photoproduct of COMb provides both a direct indication of the coordination status of the heme and a source of comparison with extensive Raman studies of the unfolding intermediates of deoxyMb.

Resonance Raman and absorption spectra of the heme and heme environment of Mb, acquired during a rapid (millisecond) pH drop[20] and pH titrations[21−24] have revealed intermediates for the low-pH unfolding of different forms of holo Mb. For deoxyMb, there is an initial intermediate, I′, in which the iron-proximal histidine bond (Fe−His) is ruptured and water has become a strong fifth ligand. Further acid-induced unfolding results in the formation of U′, in which the heme is either four-coordinate or has water coordinated as a weak fifth and sixth ligand. MetMb manifests only a U-type species. COMb, probed under the low-pH conditions that generate the deoxyMb I′ intermediate, shows a small blue shift in the Soret band (424 → 422 nm) and changes in the Raman spectra indicative of a six-coordinate CO-bound heme with a strong sixth ligand. Pulse−probe picosecond time-resolved resonance Raman[25] measurements on cryogenically trapped, low-pH forms of COMb showed that the picosecond photoproduct is essentially the same deoxyMb I′ transient species as formed during rapid-mix conditions. The result indicates that the low-pH form of COMb that has the slightly shifted Soret band has water as strong fifth ligand instead of the proximal histidine. The above picosecond Raman measurements and a transient absorption study[26] both show that there is a dramatic increase in the rate and yield of geminate rebinding associated with the low-pH form of COMb. The enhanced kinetics are consistent with the loss of histidine as a fifth ligand.

Our preliminary visible resonance Raman study[9] on encapsulated deoxyMb showed that the sol−gel can be used both to slow and limit low-pH-induced unfolding of deoxyMb, as reflected in the spectral changes at the heme. We have now added UV resonance Raman (UVRR) and fluorescence spectroscopies, as well as kinetic studies, in order to provide a more global evaluation of the conformational status of sol−gel trapped intermediates. Here, COMb is encapsulated using three different protocols, selected to provide varying efficacy in stabilization of intermediates and modulation of kinetics. In general, each encapsulated COMb sample is first exposed to unfolding conditions through a reduction in pH. The resulting low-pH forms of both COMb and any metMb that has formed are then reexposed to a buffer at near-neutral pH to induce the refolding process. Temperature variation and addition of cosolvents as well as salts are also used to further modulate the unfolding and folding processes. As the COMb changes under diverse conditions, the different spectroscopic probes are applied at specific times to monitor and characterize the generated species.

## II. Material and Methods

**Sample Preparation.** Different encapsulation protocols were used to prepare the three samples. All buffers were CO-purged before addition to the sol−gels.

Sample 1 was prepared using a variation of the original formulation of Zink and co-workers.[1] TMOS (1 mL, Aldrich) was mixed with 112 $\mu$L of deionized water and 60 $\mu$L of 2 mM HCl, and the mixture was sonicated for 30 min in an ice bath. Subsequently, 200 $\mu$L of the TMOS sol was mixed with an equal volume of a cooled, stock solution of COMb (horse skeletal, Sigma) in 50 mM potassium phosphate (KP) at pH = 6.8. The COMb−sol solution was poured into a 1.0-cm-diameter quartz NMR tube (7-in.-long). A Teflon rod with a diameter of approximately 0.9 cm was inserted into the NMR tube in order to mold the TMOS gel. Gelation occurs within a few minutes. After 2 h of aging, the Teflon mold was removed, leaving a uniformly thin and optically clear red film on the bottom one-fifth of the tube. The sample was then rinsed and covered with CO-saturated pH 6.8 KP buffer. The final concentration of the COMb in the sol−gel is ∼0.4 mM. The sample was then stored at ∼4 °C until measurements were started.

Sample 2 was prepared in an identical manner to Sample 1 except that, after sonication, 100 $\mu$L of the TMOS solution was mixed with 100 $\mu$L of a pH 6.8 PEG−glycerol solution [prepared by mixing 1.8 mL of pH 6.8 KP buffer with 200 $\mu$L of PEG (MW 400, Sigma) and 50 $\mu$L glycerol] and 200 $\mu$L of the stock COMb solution. The PEG and glycerol were added to the formulation to minimize shrinkage[27] and to possibly enhance the rigidity of the protein environment.

Sample 3 was prepared identically to Sample 2 except that the TMOS was sonicated with deionized water but without HCl.

The sample used in the fluorescence measurements and in some of the absorption measurements was prepared as a thin layer on a single optical window in a rectangular quartz cuvette. This sample was prepared without HCl and vortexed instead of sonicated, resulting in a sol−gel that we found to be highly effective in slowing conformational change in hemoglobins.

**Fluorescence Measurements.** The fluorescence emission at ambient temperature of sol−gel encapsulated COMb was obtained as a function of pH and time using front-face fluorescence[28] (SLM-AMINCO fluorimeter, Model 8100, Spectronic Instruments Inc.). The excitation wavelength was 275 nm. A sequence of spectra (from 300 to 400 nm) was generated after the replacement of the initial bathing buffer (pH 6.8) with a pH 2 buffer. When the peak position or intensity stabilized, the pH 2 buffer was replaced with a pH 7.4 buffer. The spectral changes in response to the pH increase were again monitored

over several hours. The absorption spectrum of the sample was recorded both before and after each pH change and at the end of each sequence of spectral acquisitions. In addition, the absorption spectrum was recorded 16 days after the completion of the last fluorescence measurement.

**UV Resonance Raman Spectroscopy.** The 229-nm-excited, continuous-wave (cw) UV resonance Raman (UVRR) spectra of encapsulated COMb as a function of pH and time were generated using a previously described apparatus.[29] The cooled (∼4−10 °C), sample-containing NMR tubes were both spun and rastored vertically to minimize sample heating and laser-induced degradation. The absorption spectrum of the sample was recorded before and after each sequence of UVRR measurements.

**Visible Resonance Raman Spectroscopy.** Visible resonance Raman (VRR) spectra were generated using an 8-ns pulse at 435.8 nm. The apparatus and methods for generating, detecting, and analyzing the Raman spectra were as previously reported,[30−32] except that a 0.27-m single spectrograph (Spex) with an intensified CCD detector (Princeton Instruments) was used for dispersion and detection of the Raman scattered light. The same samples were used for both VRR and UVRR measurements. The NMR tubes were spun and cooled (∼4 °C).

**Geminate Recombination.** Samples were probed once the COMb response to a solution change had ceased. A 5−7-ns pulse at 532 nm and 2 Hz (Nd:YAG, Minilite, Continuum) was used to photodissociate the CO ligand, and a 441.6-nm cw probe (He−Cd, Liconix) was used to monitor the recombination as a function of time. Geminate recombination is measured within a several hundred nanosecond time window. The details of the apparatus and data processing are described elsewhere.[30−33]

With the exception of fluorescence and some related absorption measurements, measurements were made on sol−gels cast in NMR tubes. The varied spectroscopic measurements were often made sequentially on the same sample, thus providing a more comprehensive picture of the status of the sample.

## III. Results

Each of the three samples described above was subjected to a similar set of solution changes. Spectra and kinetics were recorded at various time intervals. As a result, there is a time line of changes associated with each sample. The emphasis was primarily on obtaining a series of UV resonance Raman spectra as a function of time. After changes in the UVRR spectra ceased or slowed, the sample was usually probed using VRR and absorption spectroscopy. Less frequently, the sample was probed with respect to photodissociation quantum yield and geminate recombination. To assist in describing the time line of changes, we first present several representative spectra associated with various intermediates and end points. In this way, we can, later in the paper, present the evolution of the sample with time and in response to buffer changes without having to go into details regarding the specific spectra.

**Representative Spectra of Intermediates.** *UV Resonance Raman Spectra.* Figure 1 shows representative UVRR results for Sample 3. The series of spectra show the response of sol−gel encapsulated COMb to a series of solution conditions that are intended to cycle the protein through the unfolded state and back again to the folded state. Although UVRR spectra were collected over the Raman frequency range of ∼870 to 1670 $cm^{-1}$, the shown spectral range has been truncated to 1500−1650 $cm^{-1}$. This region is emphasized because it contains the conformationally revealing W3 and Y8a bands. The changes in the W3 band at ∼1558 $cm^{-1}$ provide a good measure of the

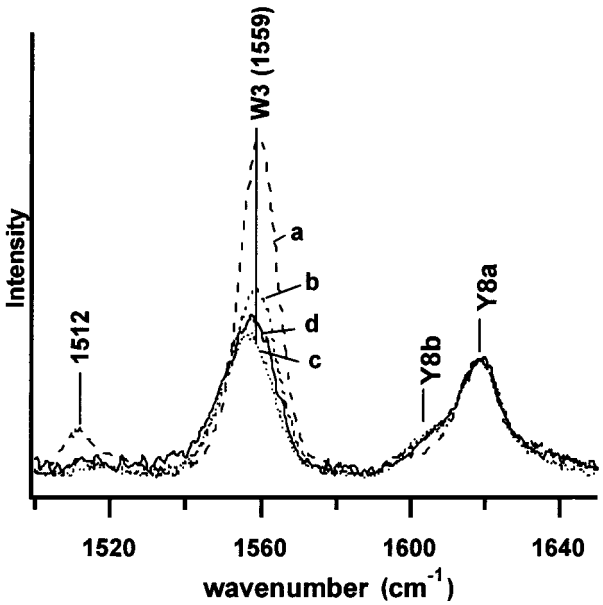


**Figure 1.** UVRR spectral results (229-nm excitation) for COMb unfolding and refolding within a sol−gel. Spectra have been normalized at the unchanging Y8a band. (a) Folded COMb. Sol−gel bathing solution is 50 mM phosphate, pH 6.8, 25% glycerol, 4 °C. Sol−gel sample is 1 day old. (b) Maximum unfolding achieved with a bathing solution of 50 mM phosphate, pH 3.0. Sol−gel is 5 days old. (c) 40 min after bathing solution changed to 50 mM phosphate, pH 1.5, room temperature. Sol−gel sample is 5 days old. Maximum unfolding. (d) Refolding achieved by raising the pH to 7.0 with 25% glycerol and warming the sample to 60 °C for 80 min. Sol−gel is 9 days old.

degree of unfolding for the A helix, where Trp A7 and Trp A14 are located, and indirectly for the adjacent E helix.[18] The Y8a band at ∼1619 $cm^{-1}$ reports on the behavior of G helix Tyr 103 and H helix Tyr 146.

The four spectra have been normalized at the Y8a peak. This peak is used for normalization because solution UVRR unfolding studies (using internal standards) of horse heart COMb (data not shown), as well as horse heart aquometmyoglobin,[18] showed that the intensity of the Y8a band remains constant over the pH range 1.5−7.5. We observed that the intensity ratios, W3/Y8a, for COMb at low and high pH are comparable for the solution phase (1.3 and 2.6, respectively) and for the sol−gel embedded (1.2 and 2.8, respectively) forms of the protein. Spectrum a is the UVRR spectrum for sol−gel embedded COMb at pH 6.8. This high-frequency region of the spectrum is dominated by the W3 peak of the A helix tryptophans. Other peaks shown are the two tyrosine-derived bands, Y8a (1619 $cm^{-1}$) and the less-intense Y8b (∼1599 $cm^{-1}$), and the unassigned 1512 $cm^{-1}$ peak. The effect of a pH decrease to 3.0 is seen in spectrum b: the cross sections of the W3 and 1512 $cm^{-1}$ bands have dramatically decreased; the W3 band has broadened and downshifted to 1558.5 $cm^{-1}$, while the Y8b band has upshifted from 1598.4 $cm^{-1}$ to 1600.0 $cm^{-1}$ and increased in intensity.

Another decrease in pH to 1.5 (spectrum c) results in changes in the W3 peak only: further intensity loss, accompanied by band broadening and a downshifting in frequency to 1557.5 $cm^{-1}$, is seen. Replacing the low-pH buffer with a buffer at neutral pH results in only partial reversal of the acid-induced changes. Spectrum d shows a UVRR spectrum from a sample that displayed the largest degree of refolding (but still not at the level of the native structure). Only W3 band changes are seen, i.e., increase of the band cross section, narrowing of the band, and upshifting of the frequency to ∼1559 $cm^{-}$.

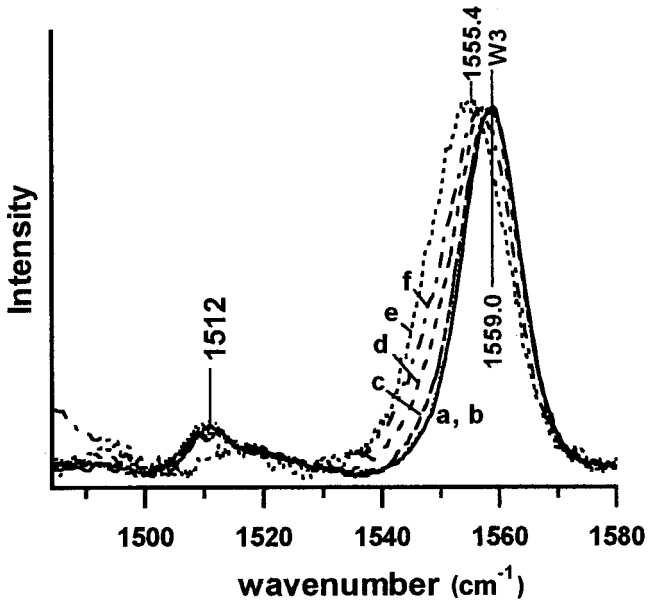


**Figure 2.** Normalized UVRR (229-nm excitation) W3 bands for COMb unfolding and refolding within a sol−gel. (a) Folded COMb. Sol−gel bathing solution is 50 mM phosphate, pH 6.8, 25% glycerol, 4 °C. Sol−gel sample is 1 day old. (b) 2 min after bathing solution changed to 50 mM phosphate, pH 3.0, 25% glycerol, 4 °C. Sol−gel sample is 3 days old. (c) 120 min after bathing solution changed to 50 mM phosphate, pH 3.0, 25% glycerol, 4 °C. Sol−gel sample is 3 days old. (d) 70 min after bathing solution changed to 50 mM phosphate, pH 3.0; sample kept at room temperature after solution change. Sol−gel sample is 4 days old. (e) 40 min after bathing solution changed to 50 mM phosphate, pH 1.5, room temperature. Sol−gel sample is 5 days old. (f) 96 min after bathing solution changed to glycerol; sample kept at room temperature after solution change. Sol−gel sample is 16 days old.

**TABLE 1: Measured Parameters for UVRR W3 Bands Given in Figure 2**[a]

| trace | fwhm | $W3/Y8_{height}$ |
|---|---|---|
| a | 11.9 | 1 |
| b | 11.7 | 1.05 |
| c | 12.6 | 0.782 |
| d | 13.9 | 0.629 |
| e | 16.2 | 0.412 |
| f | 14.8 | 0.505 |

[a] The first column lists the full-width at half-maximum, whereas the second column gives the reduced band ratio, W3/Y8, calculated using band height.

The more subtle W3 band changes that occur upon COMb unfolding and refolding are highlighted in Figure 2, where the W3 peaks for several spectra in the unfolding/refolding series for Sample 3 have been normalized. Spectrum a is the W3 band for the folded, sol−gel encapsulated COMb. The full-width at half-maximum (fwhm) for this band is 11.9 $cm^{-1}$ (Table 1, a), and its peak lies at 1559.0 $cm^{-1}$. Spectrum b illustrates that, within the first minutes after changing the pH to 3.0, there are minimal changes in either intensity (Table 1, b) or peak position. The intensity of the W3 band eventually drops relative to that of the corresponding band for the fully folded COMb. The W3 peak in spectrum c illustrates the effect of the pH 3.0 drop at an intermediate time point. Here, the band has broadened at the low-wavenumber edge (fwhm = 12.6; Table 1, c), but the peak position has not shifted. The maximum effect of the pH 3.0 drop on the W3 band is illustrated in spectrum d. The band fwhm has increased to 13.9 $cm^{-1}$ (Table 1, d), and the increase is still entirely on the low-wavenumber edge. The W3 band shift and broadening that accompany a further pH drop to 1.5 is illustrated in spectrum e. The W3 bandwidth has now increased to 16.2 $cm^{-1}$, and the peak has shifted to 1555.4 $cm^{-1}$.

Spectrum f shows the changes that occur following the replacement of the bathing buffer of Sample 3 with 100% glycerol, after the sample has undergone the pH sequence 6.8 → 3 → 1.5 → 3 → 7.0 (vide infra). The W3 bandwidth decreases to 14.8 $cm^{-1,}$ and the reduced peak ratio, W3/Y8, increases to 0.505 (Table 1, f), while the W3 peak has only upshifted to 1557.1 $cm^{-1}$. Interestingly, with the exception of spectrum e for the pH-1.5-treated COMb, the 1512 $cm^{-1}$ peak normalizes with all the W3 bands, suggesting that it is also a Trp band (see Appendix). The increased intensity at the low-frequency edge of spectrum f is due to glycerol.

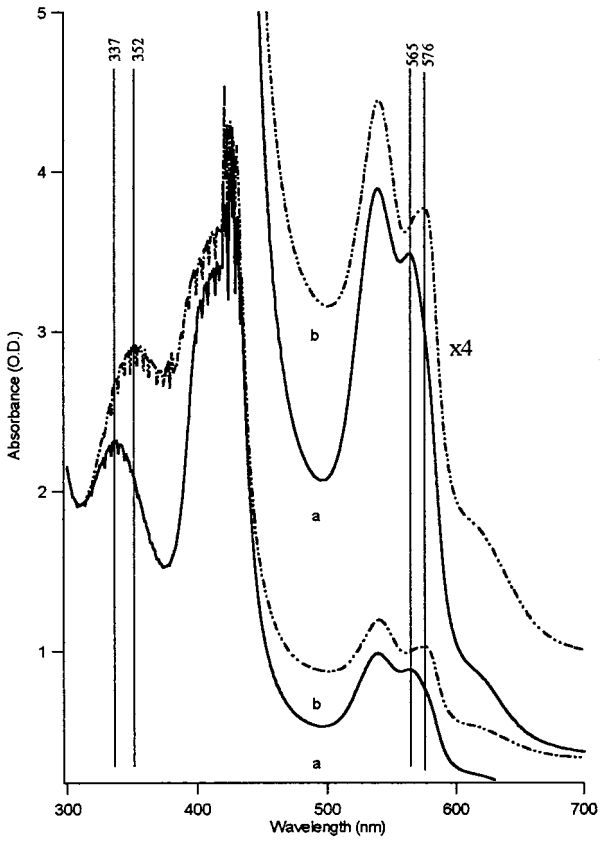


**Figure 3.** Absorption spectra of sol−gel encapsulated COMb. Trace a is of Sample 1; trace b is of Sample 2. The samples are in 100% glycerol. (Both were initially at pH 6.8 and were exposed to pH 2 prior to the change to 100% glycerol.)

*Absorption Spectra.* Figure 3 shows the visible absorption spectra of two sol−gel encapsulated COMb samples that have undergone a series of buffer changes. Spectrum a is of Sample 1. The spectrum was generated after the sample had undergone the following sequence of buffer changes: pH 6.8 → pH 2.0 → pH 6.8 → addition of 1 M NaCl → 100% glycerol. The α band in spectrum a is at 565 nm, 1 nm to the red of the 564-nm peak position of the α band for the low-pH form of COMb in solution.[20−22] Spectrum b is derived from Sample 2. It was taken after the following sequence of buffer changes: pH 6.8 → pH 2 → 100% glycerol. Spectrum b shows an α band with a peak at 576 nm, 2 nm to the blue of the 578-nm value observed for native COMb either in solution or within a sol−gel at neutral pH.[11] For both samples, the UV resonance Raman spectra obtained just prior to the absorption measurements indicate that the samples were still partially unfolded with respect to the A helix (vide infra). In these two absorption spectra, the Soret band is distorted because of saturation effects arising from the

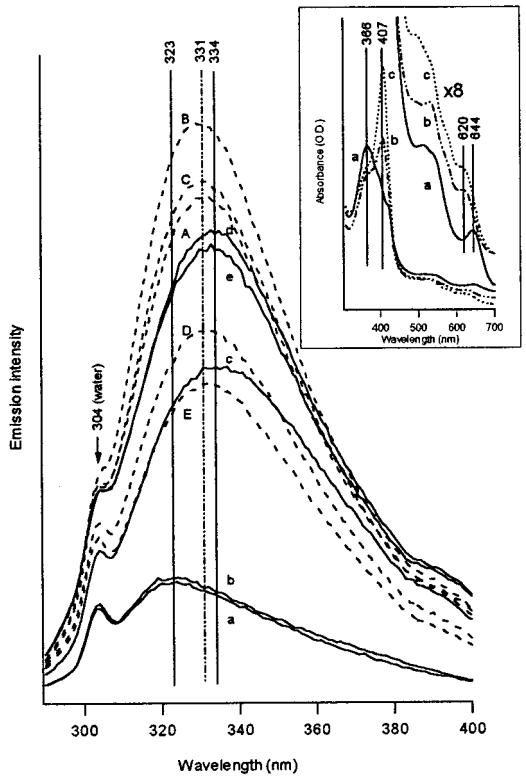


**Figure 4.** Fluorescence spectra of sol−gel encapsulated Mb. Excitation wavelength was 275 nm. A solid trace indicates either the initial folded protein at neutral pH or all scans at low pH (pH 2). A dashed trace indicates scans taken after the pH was increased from 2 to 7.4. (a) Folded COMb, pH 6.8; (b) just after change of buffer to pH 2; (c) 5 min at pH 2; (d) 15 min at pH 2; and (e) 45 min at pH 2. (A) Just after buffer change to pH 7.4; (B) 5 min at pH 7.4; (C) 10 min at pH 7.4; (D) 42 min at pH 7.4; and (E) 90 min at pH 7.4. The inset shows the corresponding absorption spectra. (a) 45 min at pH2 (just after trace e of the fluorescence); (b) 90 min after the return to pH 7.4 (just after trace E of the fluorescence); and (c) 16 days at pH 7.4.

high COMb concentration in the samples. Separate measurements on sol−gel samples with a lower COMb concentration reveal that the Soret band maximum is at 422 nm for samples that yield the 564-nm blue-shifted α band (compared with a 424-nnm Soret band for the native COMb). Nearly all of the observed species in the absorption spectra can be accounted for by varying amounts of these two well-defined CO−heme absorption spectra; i.e., one similar to spectrum b, associated with the fully intact and properly folded heme environment, that yields a Soret band at 424 nm and an α band at 578 nm, and the other similar to spectrum a, an "end point" spectrum, associated with a disrupted heme pocket, that has a 422-nm Soret band and a 564-nm α band. It is important to emphasize that there are intermediates that exhibit the "folded" heme pocket but nonetheless contain unfolded domains of the globin. We have also observed that, if one starts with encapsulated metMb at pH 2, which exhibits an absorption spectrum characteristic of the fully unfolded U state of metMb (371-nm Soret band), and then rapidly and *fully* converts it to the CO derivative at a higher pH (6.5), there is a transient (hours) absorption feature at ∼390 nm, suggestive of a five-coordinate CO-heme. After a day, the resulting spectrum fully resembles the second basis set spectrum (422-nm Soret and 565-nm α bands).

*Fluorescence Spectra.* Figure 4 shows the fluorescence emission of an encapsulated sample as a function of pH and time at ambient temperature. The solid traces are for the initial neutral pH condition and the subsequent change to a low-pH buffer. The dashed traces are for spectra taken after changing the pH from 2.0 to 7.4. Upon lowering of the pH to 2, the emission intensity increased, and the peak maximum shifted ∼11 nm to the red, reaching a maximum effect within 15 min. Although the sample started out as COMb, it rapidly became oxidized (metMb) upon the lowering of the pH. In contrast to the sol−gels cast in NMR tubes, this cuvette-based sample contained no dithionite. Upon an increase in the pH, the emission intensity transiently increased slightly, perhaps because of pH-induced changes in the gel environment that allowed for an initial further unfolding. After about 10 min, the intensity began to gradually decrease, and concomitantly the peak wavelength blue-shifted to ∼331 nm.

The inset in Figure 4 shows the corresponding absorption spectra of the metMb species that is rapidly formed upon lowering of the pH. It is clear from the absorbance spectra that, at all stages, the sample is in the met state. At pH 2, the Mb is primarily unfolded, as is evident from the characteristic peaks at 366 and 644 nm, as well as the weaker peaks at 538 and 513 nm. Raising the pH results in the appearance of peaks characteristic of native metMb; these peaks are found at 407, 620, 579, and 534 nm. However, the regeneration of a fully folded population is not complete, as can be inferred from the residual peak at 366 nm. The refolding process continued slowly at room temperature, with the 407-nm peak increasing and the 366-nm peak decreasing over a two week period (Figure 4, inset spectrum c). After the two-week period, the intensity at 407 nm had more than doubled, and the peak maximum had shifted to 409 nm.

*Visible Resonance Raman Spectra.* Figure 5 shows several representative resonance Raman spectra, reflecting the heme structure and its environment. The visible resonance Raman spectra of the evolving samples were generated at different times. At the start of each sequence of pH changes, when the sample is at near-neutral pH, the single 8-ns pulse generates a spectrum that is composed entirely of peaks derived from the five-coordinate photoproduct. Spectrum a is one such example. The spectral features that are of primary interest are the iron-proximal histidine stretching mode,[34−37] $\nu$(Fe−His), at ∼220−222 cm$^{-1}$ and the $\nu_7$ mode at 673 cm$^{-1}$. The spectra of the nanosecond photoproduct of folded COMb at neutral pH, in sol−gel using the three different protocols, are all very similar to those observed in solution (data not shown). The only exception is that the frequency of the $\nu$(Fe−His) band is increased slightly, signaling that, within the sol−gel, there is a significant slowing of the rapid, picosecond relaxation observed in solution.[38] This issue will be the focus of a future publication.

Low-pH intermediates are expected to show any of several possible Raman spectral changes.[20−25] The low-pH loss of the Fe−His bond requires an initial unfolding of the globin.[9,24] Presumably the subsequent protonation of the proximal histidine contributes to further unfolding by destabilizing the heme−histidine interaction. The low-pH unfolding intermediates typically show a $\nu_7$ band that is shifted to higher frequency (maximum shift appears to be 678 cm$^{-1}$). The loss of the iron−histidine bond in COMb results in a species that undergoes picosecond geminate recombination with high efficiency, whereas the native structure geminately rebinds with low quantum efficiency over ca. 100 ns.[25,26] As a result, the VRR spectra of low-pH COMb generated using a moderately intense 8-ns pulse will contain a sizable population of unphotolyzed COMb because of the picosecond process.

In solution studies, two unfolding intermediates have been identified for deoxyMb that have a ruptured Fe−His bond.[20−24]

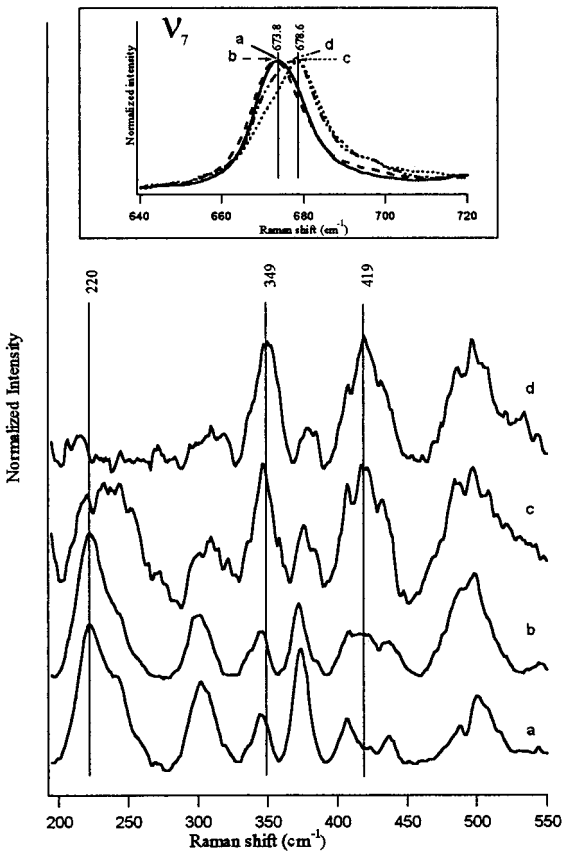


**Figure 5.** Visible resonance Raman spectra of sol−gel encapsulated COMb, generated using an 8-ns pulse at 435.8 nm. (a) Sample 1, folded COMb at pH 6.5. (b) Same sample with 100% glycerol (after exposure to buffer of pH 2). (c) Same sample at pH 7 (after exposure to pH 2 but before 100% glycerol). (d) Sample 3, at pH 7 (after exposure to pH 1.5). The inset shows the spectral region around the $\nu_7$ band.

For one intermediate, termed I′, water acting as a strong ligand replaces the histidine, and the heme remains five-coordinate. For the other intermediate, U′, the globin is more fully unfolded, and the heme is four-coordinate or weakly coordinated to two water molecules. Because the Soret absorption band for the latter is significantly blue-shifted (380 nm), it is also associated with a significant loss of resonance enhancement when using a 435.8-nm excitation wavelength. Similarly, the CO-bound heme in COMb can have histidine or water as a sixth ligand (either weak or strong) or be five-coordinate with no sixth ligand. The photoproduct of COMb at 8 ns, to the extent that a detectable photoproduct population can be generated, will reflect the coordination status of the COMb. Spectra b−d show representative VRR spectra derived from the evolving Samples 1−3 described below.

Spectra a and b (Figure 5) are both reflective of an "intact" proximal heme environment, whereas spectrum c contains a significant contribution from photoproduct that has an I′-type spectrum mixed with some photoproduct that has an intact Fe−His bond. There is also a possible contribution from the low-pH partially unfolded form[20−22] of unphotolyzed COMb. Spectrum d is completely dominated by bands arising from an I′-type photoproduct and possibly some unphotolyzed partially unfolded COMb. The $\nu_7$ bands of spectra a and b show a normal photoproduct $\nu_7$ frequency (673 $cm^{-1}$), whereas spectra c and d display a blue-shifted $\nu_7$ frequency characteristic of I′ or unphotolyzed COMb species (~678 $cm^{-1}$). At pH 2 and below, there is no detectable Raman signal, consistent with the formation of a five-coordinate COMb species and/or a U′-type

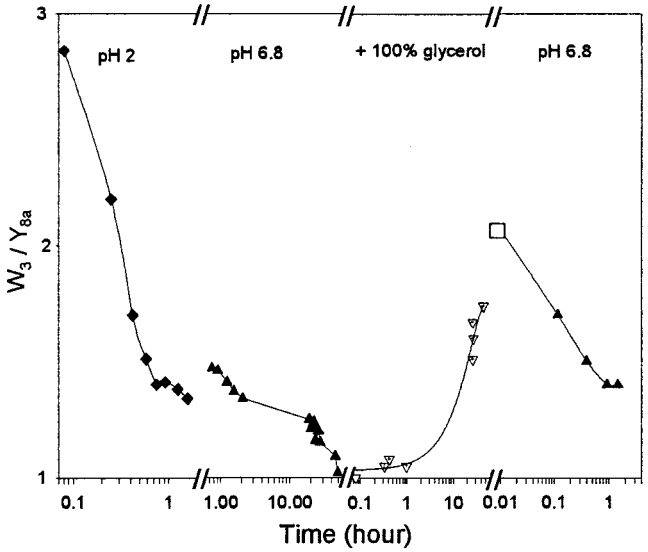


**Figure 6.** Timeline of the change in UVRR peak height ratio, W3/Y8, for Sample 1 under different bathing solution conditions (pH 2 → pH 6.8 → 100% glycerol → pH 6.8). The open square marks a measurement at 100% glycerol, just before changing the buffer pH to 6.8.

intermediate. Both species cannot yield a detectable signal with the excitation wavelength being used.

*Geminate Recombination and the Quantum Yield (QY) for Photodissociation at 8 ns.* A substantial reduction in the quantum yield of photoproduct at 8 ns, under conditions where there is no loss of COMb due to metMb formation, is taken as an indication of the loss of histidine as a sixth ligand. The observation of a sizable population of photoproduct that is undergoing geminate rebinding on the 100-ns time scale is taken as an indication of both an intact Fe−His bond and an intact distal heme pocket. In the absence of a distal heme pocket, the photodissociated ligand either rebinds within picoseconds or diffuses sufficiently far away so as to preclude the occurrence of a nanosecond-to-microsecond geminate phase. It should be noted that, in solution, there is a geminate yield of only a few percent for COMb at neutral pH,[39−41] whereas, in the sol−gel, by virtue of a slowing of the tertiary relaxation of the proximal heme pocket, there is a substantial enhancement of the geminate yield for the 100-ns rebinding process.[54] In this study, we found a direct correlation between the appearance of a $\nu$(Fe−His) band in the VRR spectrum of the photoproduct and the occurrence of both a substantial photoproduct yield and a detectable geminate phase on the 100-ns time scale.

**Time Lines for Samples 1−3.** *Time Line for Sample 1.* Sample 1 consists of COMb encapsulated with neither PEG nor glycerol. Figure 6 depicts the evolution of the W3/Y8a ratio in the UVRR spectrum of this sample. The history of the sample starts with the initial preparation in which the sample is bathed in pH 6.8 potassium phosphate buffer. The initial W3/Y8a ratio is close to 3. The VRR spectrum is essentially identical to that derived from a comparable solution-phase COMb sample. The $\nu_7$ band is at 673 $cm^{-1}$, and $\nu$(Fe−His) is clearly evident but at a slightly higher frequency (220 $cm^{-1}$ versus 218 $cm^{-1}$ in solution). The absorption spectrum consists of the normal COMb bands with an α band at 578 nm.

The first time point on the plot corresponds to the first spectrum, recorded immediately (within 5 min) after the pH was reduced to 2.0. As seen in Figure 6, the W3/Y8a ratio decreases and stabilizes over the course of 95 min to a value of approximately 1.3−1.4. During this period, the sample is

maintained at ~4 °C. After 95 min, the absorption and VRR spectra were recorded. The absorption spectrum shows the presence of a modest amount of fully unfolded metMb in addition to COMb with an α band at 568 nm. The VRR spectrum shows overall loss of intensity; an unshifted $\nu_7$ band; a reduced, but clearly discernible, unshifted $\nu$(Fe−His); and bands attributable either to the I′ photoproduct or to unphotodissociated COMb. The subsequent addition of dithionite reduced the metMb population, which resulted in an increase in the W3/Y8a ratio to 1.60.

After the pH 2 sample was stored overnight in a cold room (~4 °C), it yielded a COMb absorption spectrum with an α band at 565 nm. The VRR spectrum was greatly reduced in intensity and had insufficient signal to yield meaningful peak positions. The W3/Y8a ratio at this point was 1.47.

The buffer was then changed back to pH 6.8. Figure 6 shows that the W3/Y8a ratio did not increase but, instead, slowly decreased over the course of 2 days. During this period, the absorption spectrum barely changed: an α band was located at 566 nm. There was no evidence of significant metMb formation. The W3/Y8a ratio eventually reached a value of close to 1.0, which is characteristic of an unfolded A helix with the two A helix tryptophans (A7 and A14) both fully exposed to aqueous solvent.[18] The VRR spectrum of this species appears to be a mixture of I′ photoproduct, unphotolyzed COMb, and photoproduct with an intact but altered Fe−His bond. The $\nu_7$ band is blue- shifted to 678 cm$^{-1}$. The photodissociation and geminate rebinding measurements of this species reveal a substantial photodissociated population at 8 ns and a sizable population undergoing geminate recombination between 8 and several hundred nanoseconds.

The replacement of the bathing buffer with one containing 1.0 M NaCl (pH 7.0) caused further reduction in the W3/Y8a ratio (1.09 → 1.0) but with no change in the absorption spectrum. This observation corroborates the finding that high ionic strength favors the unfolded form of deoxyMb.[42] Surprisingly, the VRR spectrum showed an increase in the intensity of $\nu$(Fe−His) at 220 cm$^{-1}$, suggesting that, even though high ionic strength favor the unfolded globin, it nevertheless stabilizes the intact heme pocket, perhaps through osmotic effects (vide infra). The frequency of $\nu_7$ remained blue-shifted at 678 cm$^{-1}$, and the spectrum still showed indications of I′ photoproduct and possibly unphotodissociated COMb.

The bathing buffer was then replaced with an excess of CO-saturated glycerol. As can be seen in Figure 6, the W3/Y8a ratio slowly increased over several hours until it leveled off at a value of ~1.7. The absorption spectrum still exhibited a blue-shifted α band at 565 nm, and the VRR spectrum returned to that of the native species with a normal-appearing $\nu$(Fe−His) band and a $\nu_7$ band at 673 cm$^{-1}$. There was no obvious trace of I′ photoproduct or unphotolyzed COMb in the VRR spectrum. After storage for an additional 30 days at 4 °C, this sample exhibited an additional increase in the W3/Y8a ratio up to 2.07 (the open square data point) and an α band at 564 nm. Upon replacement of the glycerol with a pH 6.8 phosphate buffer, the W3/Y8a ratio again decreased over the course of hours to a value of 1.4. Both the absorption and VRR spectra remained essentially unchanged.

*Time Line for Sample 2.* Sample 2 differs from Sample 1 in that its sol−gel contains both PEG and glycerol. The initial bathing buffer is, however, the same in both instances. Figure 7 provides a time line for the evolution of the W3/Y8a ratio. At the start of the measurements, prior to the lowering of the pH, both the absorption and the VRR spectra were typical of native COMb. The frequencies of $\nu$(Fe−His) and $\nu_7$ were 222.3 and 673 cm$^{-1}$, respectively. The α band was at 578 nm. Upon the lowering of the pH from 6.8 to 2.0, the W3/Y8a ratio decreased steadily over a 1-h period but leveled off at a value near 1.3. The absorption spectrum of the sample yielded a slightly decreased wavelength of 576 nm for the α band; the VRR spectrum appeared to be dominated by the photoproduct, but the $\nu$(Fe−His) band showed reduced relative intensity and $\nu_7$ was slightly blue-shifted. There were no obvious intense signals from I′ photoproduct or unphotolyzed COMb.

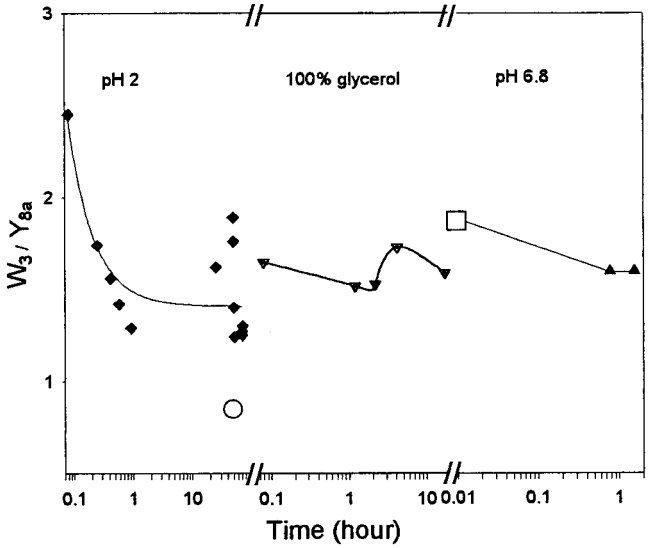


**Figure 7.** Timeline of the change in UVRR peak height ratio, W3/Y8, for Sample 2 under different bathing solution conditions (pH 2 → 100% glycerol → pH 6.8). The open circle marks a measurement just after the sample was heated to 60 °C. The open square marks a measurement at 100% glycerol, just before the buffer was changed pH to 6.8

Over the next 12 h, the W3/Y8a ratio increased slightly. Mild warming of the sample increased the value of the ratio; however, when the sample was heated at 60 °C for 3.5 h, the ratio dropped to 0.86 immediately after removal from the heat source (the open circle in Figure 7). Within a few hours after the heat treatment, the W3/Y8a ratio increased back to ~1.3. The absorption spectrum revealed an α band at 571 nm. The VRR spectrum was still very similar to the one described earlier but with a slightly more blue-shifted $\nu_7$ band (~674.5 cm$^{-1}$). The spectral features of this sample did not change with a subsequent 30-min exposure first to an ice/water bath and then to a warm water bath.

Replacement of the pH 2 buffer with CO-saturated glycerol resulted in a slight increase in the W3/Y8a ratio, which leveled off and remained stable for 4 weeks at a value of ~1.6. The α band for stable, glycerol-bathed Sample 2 was at 574.5 nm, and the VRR spectrum fully resembled spectra from the photoproduct of native COMb; the $\nu_7$ band was back at 672.4 cm$^{-1}$. After an additional one month period, the W3/Y8a ratio increased to 1.9 (open square marker in Figure 6), and the α band was red-shifted (576 nm). Replacement of the glycerol with pH 6.8 phosphate buffer resulted in a progressive decrease of the W3/Y8a ratio to 1.6, and a blue shift of the α band, first to 570 nm and eventually to 568.5 nm, where it remained stable, as shown by measurements over a period of several days.

*Time Line for Sample 3.* This sample was prepared with PEG and glycerol, as for Sample 2, but it differed from Sample 2 in that HCl was not added to the TMOS during sonication. Qualitatively, this sample exhibited the same pH- and glycerol-

dependent behavior as the previously described samples; however, it was subjected to a variety of additional solution changes chosen to provide additional insight into the nature of the unfolding and folding process within the sol−gel. These additional aspects are summarized below.

The pH drop for this sample was carried out incrementally. The initial pH 6.8 buffer was first replaced with a pH 3.0 buffer containing 25% glycerol, resulting in a modest decrease in the W3/Y8a cross-section ratio from 1.53 to 1.31 over the course of 2 h of cycling between 22 and 4 °C. The α band was observed to be at 572 nm. Changing the buffer to a glycerol-free pH 3 buffer resulted in a further drop in the W3/Y8a cross-section ratio to 1.15, but the α band actually red-shifted slightly to 576 nm. The VRR spectra from both pH 3 samples were characteristic of the five-coordinate photoproduct with the Fe−His bond intact. The $\nu_7$ band was not shifted, and the spectra were free of bands attributable to I′ photoproduct and unphotolyzed COMb. The lowering of the pH to 1.5 resulted in a UVRR spectrum that resembled the solution spectrum of pH 2 metMb.[18] The W3/Y8a cross-section ratio at this point was 0.97.

The refolding sequence was also pursued in a sequential fashion. The pH 1.5 buffer was replaced with pH 3 buffer, resulting in an increase of the W3/Y8a cross-section ratio to 1.17 and in the appearance of an α absorption band at 567 nm. The VRR spectrum was extremely weak and showed no sign of a $\nu$(Fe−His) band. The pH was then raised to 7. Although the α band shifted to 575 nm, the W3/Y8a cross-section ratio actually decreased to 0.82 over the course of several hours. The VRR spectrum was characteristic of I′ photoproduct and/or unphotolyzed COMb but resembled the spectra reported for low-pH forms of COMb. When this buffer was replaced with one at the same pH but with 25% glycerol, the W3/Y8a cross-section ratio increased to 1.15 over a period of an hour, and the VRR spectrum substantially resembled that of the five-coordinate photoproduct, revealing an intact proximal heme pocket, as reflected in $\nu$(Fe−His) and the propionate-sensitive bands. Heating to 60° C did not result in any further change in the W3/Y8a ratio. Replacement of the buffer with glycerol increased the W3/Y8a ratio to 1.3. It was observed that, when the fraction of metMb increased, the ratio dropped (1.15) but rapidly recovered to the previous value of 1.3 when re-reduced. The α band at this point was at 575 nm. The glycerol was then replaced with a 2 M ammonium sulfate solution (pH 7.1). The W3/Y8a cross-section ratio started to drop within 30 min of the buffer change and continued to decrease over the next few days, achieving a value of 1.02. Despite the drop in this ratio, the α band remained at 578 nm. A final buffer change to pH 10 produced very little change in any of the spectroscopic parameters over a period of 1.5 h.

## IV. Discussion

**Acid Unfolding of Sol−Gel Encapsulated COMb: Does Unfolding Take Place in the Sol−Gel?** Several spectroscopic indicators show that encapsulated COMb can attain, albeit much more slowly, the same unfolded state that is observed in low-pH solutions. In particular, the UVRR spectrum shows the same changes in the tryptophan bands and the same lack of change in the tyrosine Y8a band. It can be concluded that the unfolding of the A helix, and the concomitant exposure of Trp 7 and Trp 14 to solvent that is responsible for the spectral changes observed in solution,[18,19] is also occurring in the sol−gel. The substantial increase in the tryptophan fluorescence signal, with a red shift in the fluorescence maximum, for low-pH, encapsulated Mb is also consistent with this interpretation, as both of these changes are signatures for the unfolding of the tryptophan-containing helix and the exposure of the tryptophans to an aqueous environment. Some change in environment for Tyr 103 and Try 146 on the G and H helices, respectively, is signaled by the 1.5 $cm^{-1}$ upshift of the Y8b band under denaturing conditions. The absence of any indication of heme loss and the known tight templating of the sol−gel around the encapsulated protein suggest very strongly that, despite the exposure of the tryptophans to water and the disruption of the heme pocket, the acid-unfolded, encapsulated species must still retain the same general tertiary shape as the folded protein. By inference, the corresponding species in solution, which has the same spectroscopic signatures, must also retain an overall shape similar to that of the folded species.

The VRR and absorption spectra indicate substantial perturbation of the heme−heme pocket conformation. At cryogenic temperatures,[25] low-pH COMb yields the same VRR spectrum as observed in low-pH rapid-mix measurements.[20] The picosecond photoproduct at cryogenic temperatures[25] resembles I′ derived from deoxyMb at low pH under either rapid-mix[20] or equilibrium conditions.[23,24] The altered low-pH COMb VRR spectrum originating from the 2-nm-shifted Soret band resonance is consistent with a strong sixth ligand. Because the cryogenic photoproduct of this species yields an Fe−His-free VRR spectrum resembling the I′ spectrum, the most consistent picture that links these results is one in which water is the strong ligand both for I′ and for the parent low-pH COMb. It is plausible that water acts as a strong ligand because of hydrogen bonding to a nearby amino acid. Although the spectra indicate that the dominant species has water as a strong sixth ligand, there are also suggestions of a population having no sixth ligand or water bound as a weak sixth ligand, as previously noted by Champion and co-workers for solution studies.[21,22] In addition to the low-pH COMb samples that yielded no discernible VRR spectrum, evidence for such species comes from absorption measurements. The met Mb formed at low pH during the course of these measurements consistently yielded absorption spectra identical to that of the fully unfolded, four-coordinate species. This species, when converted back to the CO derivative at a higher pH, ultimately (after 1 day) yielded the CO derivative having water as a strong sixth ligand but also showed intermediate spectra (which appeared within minutes and lasted for hours after COMb formation), suggestive of either a five-coordinate CO−heme or a CO−heme with a weak sixth ligand.

**Acid Unfolding of COMb: Differences between Solution and Sol−Gel.** Although the spectroscopic signatures of unfolding appear to be very similar for the solution-phase and the sol−gel-phase Mb samples, there are differences. In solution, a pH 2 sample of Mb will typically lose the heme group after a period of time. For encapsulated Mb, even when maintained for weeks at a pH value below 2, there is never any indication of heme loss, as reflected in the appearance of free heme in the bathing buffer. This observation is consistent with the expectation that the constrained volume available to the low-pH form of the protein in the sol−gel does not allow for full unraveling of the protein. Individual helices may unfold, but the overall shape of the molecule is likely to be retained because of the boundary conditions imposed by the sol−gel matrix.

The low quantum yield for photodissociation at low pH is also an indication that the heme is still bounded by a functional, distal heme pocket that prevents the dissociated ligand from rapidly diffusing away. The low-pH form of COMb has a low potential energy barrier controlling reformation of the iron−

CO bond after photodissociation.[25,26] However, with no distal pocket to maintain the dissociated ligand in the vicinity of the iron, one would anticipate that an 8-ns excitation pulse would successfully generate a large photoproduct population. Instead, the low-pH form exhibits a very low photolysis quantum yield at 8 ns, consistent with there being a substantial picosecond rebinding process of the kind observed for low-pH COMb at cryogenic temperatures.[25,26] Thus, the low yield of photoproduct indicates both a low barrier for rebinding and an at least partially intact distal pocket.

The loss of the Fe−His linkage and an overall loosening of the heme pocket are expected to enhance heme loss even for a globin that retains a near-native fold. The complete absence of heme loss for the encapsulated Mb, despite the disruption and loosening of the heme pocket, indicates that the sol−gel acts to damp the large-amplitude structural fluctuations needed to allow for the release of even the noncovalently attached heme from the loosely folded globin.

Not all of the low-pH encapsulated samples achieved the spectroscopically determined unfolding endpoint observed in solution. Sample 2, which contained PEG and glycerol, but excluded the step of initiating hydrolysis with HCl, never yielded spectra that indicated full unfolding. It was not clear whether the population was a mix of unfolded and folded species or some pure population of an intermediate. The absorption and visible resonance Raman spectra of the sample at pH 2, together, are most consistent with a COMb species that is still easy to photodissociate and that has the iron−histidine bond intact but altered. This result suggests that the protocol used to prepare Sample 2 confers a considerable degree of protection against acid-induced unfolding. The incorporation of glycerol into the sol−gel as part of the preparative protocol for Sample 2 is likely to be at the root of this effect, given the impact that subsequently added glycerol has on the folding process (vide infra).

It is clear that, with encapsulation protocols that eventually yield spectroscopic signatures of the fully unfolded species, the pH needed to achieve this degree of unfolding is lower than that required for the same result in solution. The VRR spectrum of an encapsulated sample exposed to pH 3 buffer both with and without 25% glycerol in the bathing buffer shows no indication of the formation of COMb with a ruptured Fe−His bond. In solution, this pH is sufficiently low to produce a sizable population of COMb with the iron−histidine bond ruptured.[25,26] The sol−gel not only slows the kinetics of acid-induced unfolding but also lowers the p$K_a$ for the formation of both I′ and U′.

**Solvent and Heme-State Effects on the Acid Unfolding of Encapsulated COMb.** Changes in either the solvent or the state of the heme can modulate the stabilization of populations of acid-treated COMb in the sol−gel. It is clear that the presence of glycerol in the sol−gel greatly biases the population toward the native structure, as reflected both in the W3/Y8a ratio and in the Raman bands associated with the heme. In contrast, the addition of high ionic strength solvent, or the formation of metMb under conditions where the sample had not as yet achieved the fully unfolded state, invariably enhanced the UVRR signature ratio of unfolding. The addition of dithionite and CO to the metMb-containing samples resulted both in the reformation of COMb and in an evolution of spectroscopic features, indicating a decrease in the degree of unfolding. This result is not unexpected given that it is well established that metMb can be unfolded under higher pH conditions than COMb.

**Unfolding Intermediates and Unfolded Species.** The identification of spectroscopically distinct species along the unfolding pathway is made possible for the encapsulated COMb through the combination of the slowing of the unfolding kinetics, the decrease in the p$K_a$ of unfolding, and the ease with which the solvent environment is changed within the sol−gel. The earliest changes seen in the UVRR spectra show a decrease in the intensity of the main portion of the W3 band. The W3 band contains two slightly separated components arising from the two contributing tryptophans.[18] The peak frequency of W3 is sensitive to the dihedral angle of the indole ring.[43] The crystallographically determined dihedral angles for the tryptophans allow for the assignment of the central W3 peak to Trp A14 and the lower-frequency component to Trp A7.[18] The initial acid-induced changes are consistent with A14 becoming exposed to a more hydrophilic environment, but without any change in the dihedral angle. This finding suggests a possible loosening of the packing between the A and E helices in the region where A14 hydrogen bonds to the E helix. At this point, the heme environment is minimally perturbed, as evidenced by the VRR and absorption spectra. Subsequent changes in the UVRR spectra show a progression that leads to both a decrease in relative intensity of the entire W3 band and a shift of the entire band to a lower frequency. This final situation, similar to what was reported previously for unfolded metMb[18] and apoMb,[19] indicates both an increased exposure to water for both tryptophans and an unfolding of the A helix.

The VRR and absorption spectra indicate substantial perturbation of the heme−heme pocket conformation. There are spectra observed that are consistent with the formation of a COMb species in which the proximal histidine is replaced by water as a strong sixth iron ligand.[20] Although the spectra indicate that the dominant species has water as a strong sixth ligand, presumably because of hydrogen bonding of the water to a nearby amino acid residue, there are also suggestions of a population having no sixth ligand or water bound as a weak sixth ligand, as previously noted by Champion and co-workers for solution studies.[21,22] In addition to the low-pH COMb samples that yielded no discernible VRR spectrum, evidence for such species comes from absorption measurements. The metMb formed at low pH during the course of these measurements consistently yielded absorption spectra identical to that of the fully unfolded, four-coordinate species. When converted back to the CO derivative at a higher pH, the metMb ultimately (after 1 day) yielded the CO derivative having water as a strong sixth ligand but also showed intermediate spectra (which appeared within minutes and lasted for hours after COMb formation), suggestive of either a five coordinate CO−heme or a CO−heme with a weak sixth ligand.

**Refolding of Sol−Gel Encapsulated COMb.** The reexposure of an aged (several days) acid-unfolded, encapsulated COMb to buffer at neutral pH does not result in a rapid refolding of the protein. The lack of refolding may be related to the fact that sol−gels continue to cross-link for days after the gel first begins to form. The samples that remained under low-pH conditions for days may undergo a retemplating of the encapsulation cavity, thereby enhancing the stability of the unfolded conformation. The one exception to this observation was for the sample used in the fluorescence measurements. In that case, the sample was maintained at low pH for only a few hours, and the changes in fluorescence clearly show that the sample substantially evolved back toward the native structure. Nevertheless, the full refolding process in this case is still very slow. The changes in the absorption spectrum (for the sample used in the fluorescence studies) continued over a period of many days.

The fact that, with increasing pH, low-pH unfolded samples typically underwent further unfolding of the A helix, as reflected in the changes in the W3/Y8a ratio, suggests that, once the A helix is unfolded and water-exposed, the sol−gel environment seems to actually favor the unfolded A helix. A possible explanation is that the sol−gel has slowly evolved (vide supra) in a way that stabilizes a configuration of water molecules that hydrate the unfolded A helix. If so, then the sol−gel has, in effect, formed a template for the hydrated unfolded A helix, thus making it energetically costly to refold the A helix in the presence of water. Another possible explanation for the observation of only limited refolding in the sol−gel is that, once unfolded, the COMb becomes "entropically" trapped such that unfolded segments occupy channels connecting the cavity in which the molecule was first encapsulated.[44,45]

**Effect of Glycerol on the Refolding Process.** Samples 1 and 3 both remain unfolded when re-exposed to neutral-pH aqueous buffer. The subsequent addition of glycerol initiates a slow but clear-cut evolution of spectral changes, which indicate that the tryptophan environment is not only becoming more hydrophobic (increase in the W3/Y8a ratio) but is also undergoing a refolding process, as signaled by an upshift in frequency of the W3 band. Furthermore, the addition of glycerol results in a relatively rapid recovery of spectral signatures of a native or near-native heme−heme pocket conformation. Prior to the addition of glycerol, the VRR spectra contained substantial contributions from the I′ photoproduct and what appears to be a small population of photoproduct manifesting a perturbed iron−proximal histidine linkage. Following the addition of glycerol, even at the 25% level, the yield of photoproduct is rapidly and greatly increased, and a near-normal photoproduct spectrum is observed. This "normal" photoproduct spectrum appears very early with respect to the glycerol-induced time evolution of the A helix toward its native state.

If the glycerol is replaced with nonacidic aqueous buffer prior to the complete recovery of the A helix, the UVRR spectra shows that the A helix evolves back toward its fully unfolded configuration. The heme pocket, however, remains intact. It would therefore appear that, under conditions in which the A helix is partially unfolded, this helix is very vulnerable to stresses that promote further unfolding. Eventually, the glycerol-free system stabilized with the A helix unfolded (as reflected in the UVRR) but with the heme and heme environment intact with respect to the proximal histidine and the heme propionates. Thus, at neutral pH, once the heme environment returns to its native state, it is resistant to disruption even when the A helix reverts back to being completely unfolded.

**Role of Water.** The changes induced by the addition and removal of glycerol suggest that water plays a key role in the folding and unfolding pathways. The role of water is supported through kinetic studies on a series of mutant myoglobins,[24,46] in which the unfolding rates, measured as a function of hydrophobicity of the distal heme pocket, show that heme-pocket water plays a key role in the unfolding process.

The VRR spectra of encapsulated samples that had been cycled from pH 2 back to neutral pH, show evidence for an equilibrium between populations having a distorted Fe−His linkage and those with water as a strong heme ligand (I′). The addition of glycerol pushes that mixed population to one that has an intact Fe−His linkage and spectral signatures of a native heme pocket. Once formed, this configuration of the heme pocket remains stable at neutral pH, even when significant additional unfolding of the A helix follows. It is very likely that a major component of the kinetic barrier for the reformation of the native heme pocket is the removal of both the tightly liganded water and the excess, loosely bound water from the heme environment. These waters are likely to prohibit the F helix from shifting sufficiently to allow for the now-deprotonated proximal histidine to form the stable Fe−His bond associated with the native structure. It is also likely that an iron-coordinated water is reasonably stable under conditions in which the A helix is still unfolded and the proximal histidine is not protonated. It is plausible that the deprotonated histidine contributes to making the water a strong ligand through a hydrogen bond. Thus, at neutral pH under conditions in which the A helix is partially or fully unfolded, the I′ heme-pocket configuration and the intact heme-pocket configuration have comparable stability but are separated by a kinetic barrier that requires disruption of the Fe−His bond to form I′ or, for the reverse process, a removal of liganded water to form the native configuration. The results suggest that the addition of glycerol osmotically destabilizes I′, thus lowering the barrier for the I′ → N transition in the heme pocket (N being the native heme-pocket structure).

**Folding and Unfolding Pathways.** The pH-folding intermediates spectroscopically identified at neutral pH in this study include species that have the A helix unfolded but the heme pocket either intact or disrupted. The results certainly suggest that the A helix is the last element of the structure to refold and that partial disruption of this helix facilitates further unfolding by creating conditions that facilitate the introduction of water into the heme pocket. It is plausible that perturbations that expose a certain domain of the A helix to water initiate progressive destabilization of the entire helix. Glycerol can seemingly exert sufficient osmotic stress to reverse this effect, but once the glycerol is removed, unfolding of the helix resumes. Assuming this effect is not a purely sol−gel-induced phenomenon, this scenario would also suggest that the unfolding pathway in solution might follow a similar mechanism, in which the unraveling of the A helix leads to a sequential destabilization of other domains, which are then able to respond to the presence of denaturants and water. Thus, the role of denaturants such as protons would be two-fold: unfolding the A helix and stabilizing unfolding intermediates associated with the heme pocket such as I′. As discussed earlier, the second component can only occur once the A helix has become disrupted. This leads to the prediction that the sol−gel-stabilized refolding intermediate that has the unfolded or partially unfolded A helix but an intact proximal heme pocket should undergo loss of the iron−histidine bond and further heme-pocket unfolding under much milder (e.g., higher pH) denaturing conditions than for the starting native species.

An intermediate with a segment of the A helix exposed to water and partially unfolded, but with the rest of the protein intact, is supposedly created during the burst phase of the unfolding process for apoMb.[47,48] If so, then the COMb structure generated in the sol−gel through the series of solvent changes that has the intact heme environment but an unfolded or partially unfolded A helix is likely to be the intermediate produced during the burst phase of unfolding. Far UVRR or FTIR studies of amide bonds in this species are needed to more fully characterize the degree to which the helices are perturbed.

## Conclusion

The present study shows that sol−gel encapsulation of COMb, in combination with a variety of solvent cycling protocols, can be used to trap and characterize not only the acid-unfolded species observed in solution, but also several partially unfolded species that are plausible unfolding and folding

intermediates. The results directly support the view that the unfolding and increased exposure to solvent of at least some segment of the A helix is the initial step in the unfolding pathway. In addition, the results indicate that the refolding of the A helix is likely to be the last process in the refolding pathway. The ability of the sol−gel both to trap these intermediates and to slow the kinetics of unfolding and refolding opens the door for detailed studies of the burst phase that is typically too fast to easily monitor using conventional techniques.[47,48] The present study also indicates that different encapsulation protocols confer differing degrees of stability to encapsulated proteins. It appears that the inclusion of PEG and glycerol into the sol−gel formulation is a step in the direction of producing highly robust protein-based biosensors.

## Appendix

**Assignment of the 1512 cm$^{-1}$ Peak.** The concomitant decrease in the W3 and 1512 cm$^{-1}$ bands, as illustrated in Figure 1, strongly suggests that the latter unassigned band can be attributed to tryptophan. This assumption is supported by the UVRR results for a deoxyhemoglobin mutant, Hb$\beta$W37E, in which both the low-frequency W3 shoulder of Trp$\beta$37 and the 1512 cm$^{-1}$ peak are absent (unpublished results). Both of these peaks are found in the UVRR spectrum of human deoxyHb, but only the 1512 cm$^{-1}$ band decreases upon CO ligation.

In the case of Mb unfolding, the excitation profile of Trp is blue-shifted away from the 229-nm excitation wavelength as the Trp environment becomes more polar, resulting in a decrease of the Trp Raman cross section.[18] It seems plausible that, for the T → R transition in hemoglobin, in which ligation at the heme induces a separation of the subunits at the $\alpha_1\beta_2$ interface and Trp$\beta$37 becomes more solvent exposed, a similar blue shifting of the Trp$\beta$37 excitation profile occurs. The spectral consequence of the breaking of the hydrogen bond between Trp$\beta$37 and Asp$\alpha$94 during the T → R transition in hemoglobin most likely contributes.

Other data in the literature suggest that modes involving indole $N_1H$ motion contribute to the 1512 cm$^{-1}$ band. This band is not found in the 229-nm-excited UVRR spectrum of an aqueous solution of Trp $d_5$, yet it appears in the spectrum of a recombinant deoxyHb in which all Trps are replaced with Trp $d_5$.[49] These results are consistent with assignment of the 1512 cm$^{-1}$ band to environmentally sensitive $N_1H$ modes.[50,51] Lautie et al. acquired the Raman spectra (excitation at 641 nm) of molten indole (70 °C) and four deuterated indoles: d-2; $d_2$-1,3; $d_4$; and $d_7$.[52] In this hydrophobic environment, the indole UVRR spectrum yields a very strong band at 1506 cm$^{-1}$. Two other deuterated indoles, d-2 and $d_4$, neither of which is deuterated at $N_1H$, yield UVRR bands at 1506 and 1502 cm$^{-1}$, respectively. When the indole becomes N-deuterated, the strong ∼1506 cm$^{-1}$ band downshifts: for $d_2$-1,3, to 1491 cm$^{-1}$; and for $d_7$, to 1451 cm$^{-1}$.

The 1512 cm$^{-1}$ band for deoxyHb also downshifts by 5 cm$^{-1}$ in $D_2O$, resulting from H/D exchange at the indole $N_1H$.[49] Assignment of the 1512 cm$^{-1}$ band to a 2×W18 mode was therefore disproved, as this assignment would require a 10 cm$^{-1}$ downshift.[49]

$N_1H$ motion contributes to the indole W17 and W29 modes.[50,51] W17 is a mixed mode of a benzene vibration and $N_1H$ motion, whereas W29 is the indole out-of-plane bending mode modified by $N_1H$ motion. Both modes are sensitive to environment; the W17 mode has been proposed as a probe for Trp environment.[50,51,53] The W17 mode for skatole, which is a better model for Trp than indole, has been observed at 886 cm$^{-1}$ in carbon disulfide, at 879 cm$^{-1}$ in benzene, and at 877 cm$^{-1}$ in dioxane, whereas the W29 mode is calculated to fall at 634 cm$^{-1}$.[50] A combination of these two environmentally sensitive $N_1H$ modes could yield a 1512 cm$^{-1}$ band in Hb or Mb under hydrophobic conditions; under hydrophilic conditions, the bands would be expected to disappear because of a shifting of the Trp excitation profile and to downshift in frequency when the indole $N_1$ was deuterated. This assignment of the 1512 cm$^{-1}$ band to a combination of the W17 and W29 modes is supported by the data cited above.

## References and Notes

(1) Ellerby, L. M.; Nishida, C. R.; Nishida, F.; Yamanaka, S. A.; Dunn, B.; Valentine, J. S.; Zink, J. I. *Science* **1992**, *255*, 1113.
(2) Braun, S.; Shtelzer, D.; Avnir, D.; Ottolenghi, M. *J. Non-Cryst. Solids* **1992**, *148*, 739.
(3) Avnir, D.; Braun, S.; Lev, O.; Ottolenghi, M. *Chem. Mater.* **1994**, *6*, 1605.
(4) Yamanaka, S. A.; Nishida, F.; Ellerby, L. M.; Nishida, C. R.; Dunn, B.; Valentine, J. S.; Zink, J. I. *Chem. Mater.* **1992**, *4*, 495.
(5) Wu, S.; Ellerby, L. M.; Cohan, J. S.; Dunn, B.; El-Sayed, M. A.; Valentine, J. S.; Zink, J. I. *Chem. Mater.*q **1993**, *5*, 115.
(6) Dave, B. C.; Miller, J. M.; Dunn, B.; Valentine, J. S.; Zink, J. I. *J. Sol−Gel Sci. Technol.* **1997**, *8*, 629.
(7) Edmiston, P. L.; Wambolt, C. L.; Smith, M. K.; Saavedra, S. S. *J. Colloid Interface Sci.* **1994**, *163*, 395.
(8) Akbarian, F.; Lin, A.; Dunn, B. S.; Valentine, J. S.; Zink, J. I. *J. Sol−Gel Sci. Technol.* **1997**, *8*, 1067.
(9) Das, T. K.; Khan, I.; Rousseau, D. L.; Friedman, J. M. *J. Am. Chem. Soc.* **1998**, *120*, 10268.
(10) Zheng, L.; Brennan, J. D. *Analyst* **1998**, *123*, 1735.
(11) Lan, E.; Dave, B.; Fukuto, J.; Dunn, B.; Zink, J.; Valentine, J. *J. Mater. Chem.* **1999**, *9*, 45.
(12) Shibayama, N.; Saigo, S. *J. Mol. Biol.* **1995**, *251*, 203.
(13) Bettati, S.; Mozzarelli, A. *J. Biol. Chem.* **1997**, *272*, 32050.
(14) Shibayama, N.; Saigo, S. *J. Am. Chem. Soc.* **1999**, *121*, 444.
(15) Shibayama, N. *J. Mol. Biol.* **1999**, *285*, 1363.
(16) Das, T.; Khan, I.; Rousseau, D.; Friedman, J. *Biospectroscopy* **1999**, *5*, S64.
(17) Juszczak, L.; Friedman, J. *J. Biol. Chem.* **1999**, *274*, 30357.
(18) Chi, Z.; Asher, S. *Biochemistry* **1998**, *37*, 2865.
(19) Chi, Z.; Asher, S. *Biochemistry* **1999**, *38*, 8196.
(20) Han, S.; Rousseau, D. L.; Giacometti, G.; Brunori, M. *Proc. Natl. Acad. Sci. U.S.A.* **1990**, *87*, 205.
(21) Sage, J.; Morikis, D.; Champion, P. *Biochemistry* **1991**, *30*, 1227.
(22) Sage, J.; Li, P.; Champion, P. *Biochemistry* **1991**, *30*, 1238.
(23) Palaniappan, V.; Bocian, D. *Biochemistry* **1994**, *33*, 14264.
(24) Tang, Q.; Kalsbeck, W.; Olson, J.; Bocian, D. *Biochemistry* **1998**, *37*, 7047.
(25) Iben, I.; Cowen, B.; Sanchez, R.; Friedman, J. *Biophys. J.* **1991**, *59*, 908.
(26) Miers, J.; Postlewaite, B.; Cowen, G.; Roemig, I.-Y.; Lee, S.; Dlott, D. *J. Chem. Phys.* **1991**, *94*, 1826.
(27) Wambolt, C.; Saavedra, S. *J. Sol−Gel Sci. Technol.* **1996**, *7*, 53.
(28) Hirsch, R. *Methods Enzymol.* **1994**, *232C*, 231.
(29) Juszczak, L.; Hirsch, R.; Nagel, R.; Friedman, J. *J. Raman Spectrosc.* **1998**, *29*, 963.
(30) Peterson, E. S.; Friedman, J. M. *Biochemistry* **1998**, *37*, 4346.
(31) Peterson, E.; Chien, E.; Sligar, S.; Friedman, J. *Biochemistry* **1998**, *37*, 12301.
(32) Huang, J.; Juszczak, L. J.; Peterson, E. S.; Shannon, C. F.; Yang, M.; Huang, S.; Vidugiris, G. V. A.; Friedman, J. M. *Biochemistry* **1999**, *38*, 4514.
(33) Gottfried, D.; Peterson, E.; Sheikh, A.; Yang, M.; Wang, J.; Friedman, J. *J. Phys. Chem.* **1996**, *100*, 12034.
(34) Argade, P.; Sassaroli, M.; Rousseau, D.; Inubushi, T.; Ikeda-Saito, M.; Lapidot, A. *J. Am. Chem. Soc.* **1984**, *106*, 6593.
(35) Rousseau, D. L.; Friedman, J. M. In *Biological Applications of Raman Spectroscopy*; Spiro, T. G., Ed.; John Wiley & Sons: New York, 1988; Vol. III.
(36) Kitagawa, T. In *Biological Application of Raman Spectroscopy*; Spiro, T. G., Ed.; John Wiley & Sons: New York, 1988; Vol. III.
(37) Ahmed, A.; Campbell, B.; Caruso, D.; Chance, M.; Chavez, M.; Courtney, S.; Friedman, J.; Iben, I.; Ondrias, M.; Yang, M. *Chem. Phys.* **1991**, *158*, 329.
(38) Findsen, E.; Scott, T.; Chance, M.; Friedman, J.; Ondrias, M. *J. Am. Chem. Soc.* **1985b**, *107*, 3355.

(39) Alpert, B.; El Mohsni, S.; Lindqvist, L.; Tfibel, F. *Chem. Phys. Lett.* **1979**, *64*, 11.
(40) Duddell, D.; Morris, R.; Richards, J. *J. Chem. Soc., Chem. Commun.* **1979**, *2*, 75.
(41) Friedman, J. M.; Lyons, K. B. *Nature* **1980**, *284*, 570.
(42) Tang, Q.; Kalsbeck, W.; Bocian, D. *Biospectroscopy* **1997**, *3*, 17.
(43) Miura, T.; Takeuchi, H.; Harada, I. *J. Raman Spectrosc.* **1989**, *20*, 667.
(44) Slater, G.; Wu, S. *Phys. Rev. Lett* **1995**, *75*, 164.
(45) Liu, L.; Li, P.; Asher, S. *Nature* **1999**, *397*, 141.
(46) Hargrove, M.; Krzywda, S.; Wilkinson, A.; Dou, Y.; Ikeda-Saito, M.; Olson, J. *Biochemistry* **1994**, *33*, 11767.
(47) Feng, H.; Ha, J.-H.; Loh, S. *Biochemistry* **1999**, *38*, 14433.
(48) Jamin, M.; Yeh, S.-R.; Rousseau, D.; Baldwin, R. *J. Mol. Biol.* **1999**, *292*, 731.
(49) Hu, X.; Spiro, T. G. *Biochemistry* **1997**, *36*, 15701.
(50) Harada, I.; Takeuchi, H. In *Spectroscopy of Biological Systems.*; Clark, R. a. H., Ed.; John Wiley & Sons: New York, 1986.
(51) Takeuchi, H.; Harada, I. *Spectrochim. Acta* **1986**, *42A*, 1069.
(52) Lautie, A.; Lautie, M.; Gruger, A.; Fakhri, S. *Spectrochim. Acta* **1980**, *36A*, 85.
(53) Kitagawa, T.; Azuma, T.; Hamaguchi, K. *Biopolymers* **1979**, *18*, 451.
(54) Khan, I.; Friedman, A. J.; Dantsker, D.; Friedman, J. M., manuscript in preparation.